QUARTERLY OF APPLIED MATHEMATICS
VOLUME LXXV, NUMBER 1
MARCH 2017, PAGES 19–37
http://dx.doi.org/10.1090/qam/1446
Article electronically published on August 1, 2016

A BISTABLE BELIEF DYNAMICS MODEL FOR RADICALIZATION WITHIN SECTARIAN CONFLICT

By

YAO-LI CHUANG (*Department of Mathematics, California State University at Northridge, Northridge, California 91330 — and —Department of Biomathematics, UCLA, Los Angeles, California 90095-1766*),

MARIA R. D'ORSOGNA (*Department of Mathematics, California State University at Northridge, Northridge, California 91330 — and — Department of Biomathematics, UCLA, Los Angeles, California 90095-1766*),

AND

TOM CHOU (*Departments of Biomathematics and Mathematics, UCLA, Los Angeles, California 90095-1766*)

Abstract. We introduce a two-variable lattice model to describe conflict within communities. Our model includes polarization and radicalization of individuals, each of which harbors a continuous belief variable and a discrete radicalization level describing their tolerance to others. A novel feature of our work is the incorporation of a bistable radicalization process that models memory-dependent social behavior and that may explain contradicting observations on the role of social segregation in exacerbating or alleviating conflicts. We further include institutional influence, such as through propaganda or education, and examine its effectiveness. In some parameter regimes, we find that institutional influence may suppress radicalization and allow for social conformity and appeasement over time. In other cases, institutional intervention may be counterproductive and exacerbate the spread of radicalization within a non-homogeneous population. In such instances, our analysis implies that social segregation may be a viable option against sectarian conflict.

1. Introduction. Recent years have seen the resurgence of ethnic, religious and racial tension that have created rifts among communities once at peace. In many cases, friction has escalated towards violent conflict, ethnic cleansing and at times even full-

Received May 2, 2016.
2010 *Mathematics Subject Classification.* Primary 91D10, 34C28, 62H30.
This work was made possible by support from grants ARO W1911NF-14-1-0472, ARO MURI W1911NF-11-10332, and NSF DMS-1516675.
E-mail address: yaoli.chuang@csun.edu
E-mail address: dorsogna@csun.edu
E-mail address: tomchou@ucla.edu

fledged civil wars that have destabilized entire social and political systems [4, 5, 8, 19, 21, 25, 29, 32]. The development of viable intervention strategies to mitigate radicalization and violence requires a thorough understanding of the mechanisms underlying sectarian conflict. Identifying the basic ingredients that lead to the emergence of full scale conflict is hindered by the complex nature of human behavior. Instead of simplistic, universal interpretations and solutions, one is often left with contradictory observations and outcomes.

In particular, there is controversy as to whether social segregation should be employed to manage sectarian conflicts [5, 11]. Some studies suggest that inter-ethnic or inter-communal contacts raise tension and that it is beneficial to keep rival communities separate until tensions dissipate [4, 8, 19, 25, 27, 29, 32]. Others have concluded that ethnically mixed environments encourage inter-ethnic friendship and trust, while segregation leads to prejudice and antagonistic behavior [4, 5, 11, 21, 28]. These contradicting conclusions reveal the context-dependent nature of human social behavior.

The goal of this paper is to present a mathematical framework that may help resolve basic observations of belief dynamics, radicalization, and conflict. Social studies have shown that humans often hysteretically change behaviors, perceiving and reacting to the same information in drastically different ways because of different past experiences and circumstantial contexts. Such a change of behaviors also applies to general tolerance towards others and their views. Similar socio-economic environments in some cases have led to peaceful coexistence between communities, in others to conflict. Within the context of radicalization we model this hysteresis using a memory-dependent or "bistable" response to the social environment [22, 23]. To quantify this mode-switching behavior, we draw inspiration from the physical sciences, where bistability is ubiquitous; for example, in ferromagnetism where materials switch their magnetic alignment as an external field is varied [6].

Fig. 1(a) depicts the hysteresis curve of a system in which a bistable state variable ρ (y-axis) is driven by an independent regulating variable σ (x-axis). The curve represents the equilibrium solution to, e.g., a differential equation for ρ in which σ is a controlling parameter. The solid parts of the curve indicate stable values of ρ, while the dashed segment are unstable solutions. The functional dependence of ρ on σ yields a window of values $D < \sigma < E$ in which two stable solutions can arise.

Within the context of belief/radicalization dynamics depicted in Fig. 1(a), ρ represents the degree of radicalization of a population or an individual that is driven by the social tension σ. An interesting and frequently observed phenomenon is that of a slowly deteriorating political, economic or social situation (increasing σ) which seems under control but abruptly escalates. The lower solid curve in Fig. 1(a) indicates a less radicalized population (low ρ) that favors peaceful coexistence with others of different views. Increasing social tension can force ρ to transition from the lower to the upper solid curve at $\sigma \geq E$. The upper curve represents a highly radicalized population that is non-tolerant towards those with different views. The "bifurcation point" E thus marks a sudden escalation of sectarian conflict which can be triggered by random events. Once the situation escalates, it is often very difficult to restore peace, as ρ remains on the upper solid curve even if σ is decreased back below E. Peace can only be restored if sufficient effort is made

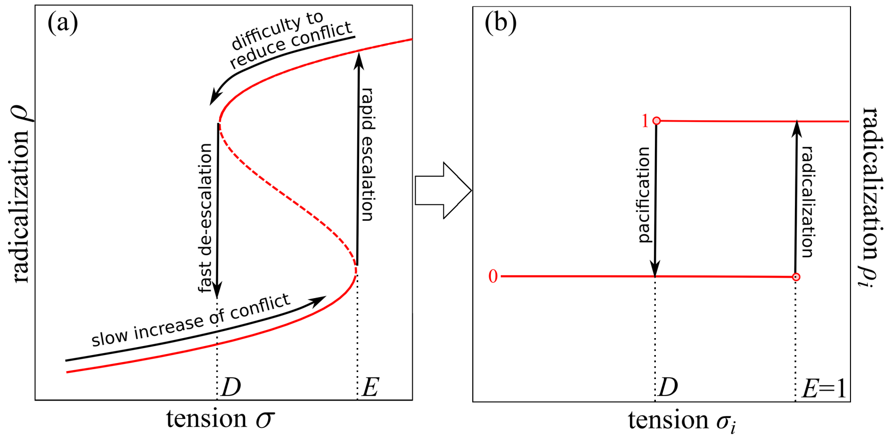

FIG. 1. (a) A typical bistability curve. The curve qualitatively captures the essence of escalating conflicts and radicalization ρ due to rising tension σ. Bifurcation values of the tension σ are labelled D (de-escalation) and E (escalation). (b) A simplified piecewise constant description of the bistable dependence of ρ_i on σ_i.

to further reduce σ below the lower bifurcation point $D < E$. The hysteresis between high and low radicalization levels may help shed light on contradicting reports regarding whether the promotion of ethnic mixing or segregation is the best approach to achieve a state of peaceful coexistence depending on the tension levels as shown in Fig. 1(a). Just like tension can rapidly escalate, it may also rapidly de-escalate. One example might be the decades-long Northern Ireland conflict. As late as 1993, some scholars were still very pessimistic on a possible peaceful resolution of the Catholic/Protestant conflict, stating that: "the cruel conflict will continue, apparently with no end in sight..." [11, 27]. However the 1994 IRA ceasefire quickly lead to the 1998 signing of the Good Friday Agreement, marking the end of "the Troubles". To incorporate bistability in a mathematically treatable way we can, without loss of generality, adopt a simplified description of the relationship between radicalization and tension, as shown in Fig. 1(b).

To understand the influence of behavioral memory on the spread of radicalization and conflict, we use the mathematical framework of DeGroot, which describes an individual's belief as a one-dimensional continuous variable bounded by two extreme limits [10, 15, 16]. Over time, individuals may change their opinions by interacting with others. In the DeGroot model, originally introduced to study the formation of consensus opinions in a network, conformity is the only ensured outcome. The inability to form heterogeneous distributions of opinions, or "persistent disagreement", limits the applicability of the model to ethnically or ideologically divergent societies [1, 2, 12, 34]. Extensions of the DeGroot model have been proposed to induce disagreement, such as the popular "bounded confidence" model, where individuals interact only with those holding similar opinions, defined by an opinion range called the bounded confidence [9, 13, 14, 20, 33].

Another approach is taken via "opinion opposition" models that introduce agents of "non-conformity" who adopt contrarian views and cause polarized beliefs and disrupt the formation of consensus [12, 18]. Such models share similarities with spin glass Ising models that describe a mixture of ferromagnetic and antiferromagnetic molecules; the former tend to align their spins with neighbors, while the latter anti-align. Since sectarian conflicts usually arise and progress through direct conflict of opinion, we will adopt an opinion opposition approach rather than a bounded confidence approach. The novelty of our work is that, assuming that opinion differences among individuals cause tension, the ensuing radicalization of an individual follows a bistable pattern as described in Fig. 1(a).

We note that relatively peaceful, albeit tense, coexistence between communities of different backgrounds can be ensured by a strong or influential player, such as the state, a dictator, inter-communal institutions, or the international community. The removal of such a player correlates with outbreaks of violent conflicts [7, 11, 17, 32]. Thus, we will also incorporate the influence of a central figure, modeled as a globally connected player exerting institutional influence similar to the concept of media influence on locally connected networks [31].

In the next section, we present the details of our basic lattice model of radicalization and sectarian conflict. We then augment the basic model to include government propaganda and explore how it influences conflict. One of our aims is to use our model to inform strategies that can stop radicalization and sectarian violence from spreading among an ethnically mixed population without employing population segregation as a peace-keeping method. Results of our analysis will be presented in the Results and Discussion Section, where parameter dependence will also be explored.

2. Bistable lattice model of conflict. We assume a two-dimensional $N \times N$ site lattice model where each site i is populated by an agent. Two dynamical variables are associated with each agent: a continuous "belief" variable $-1 \leq \phi_i(t) \leq 1$ indicating the fervor of agent i towards his or her belief, and a discrete "radicalization" variable $\rho_i(t) \in \{0, 1\}$ indicating the intolerance of agent i towards others with different beliefs. Since radicalization usually leads to conflict, we will use the two concepts interchangeably: radicals cause conflict; non-radicals allow for peaceful coexistence. We divide the population into blue ($\phi_i < 0$) and red ($\phi_i > 0$) groups and refer to them as two distinct sects. The two extreme belief values $\phi_i = -1$ and $\phi_i = +1$ (in dark blue and red respectively), represent zealot individuals, while lighter colors indicate moderates as shown in Fig. 2(a). Finally, we assume a fully occupied periodic lattice without empty sites, and that the occupying agents do not migrate.

The values $\phi_i(t)$ and $\rho_i(t)$ evolve over time via nearest-neighbor interactions. Nearest neighbors are defined using the "Moore neighborhood", where eight grid sites surrounding site i are considered, as shown in Fig. 2(b). In the following subsections we describe the model that governs the evolution of $\phi_i(t)$ and $\rho_i(t)$.

2.1. *Belief and radicalization.* The magnitude of belief $|\phi_i|$ measures the level of fervor of agent i. Individuals with $|\phi_i| \approx 1$ are belief zealots while those with $|\phi_i| \approx 0$ are belief apathetics. In addition, a discrete radicalization variable $\rho_i \in \{0, 1\}$ describes how an agent perceives other beliefs. An intolerant individual at site i will be assigned $\rho_i = 1$ and be referred to as a radical. Conversely, a tolerant non-radical will be described by $\rho_i = 0$. It is important to note that within the context of our model, ϕ and ρ describe

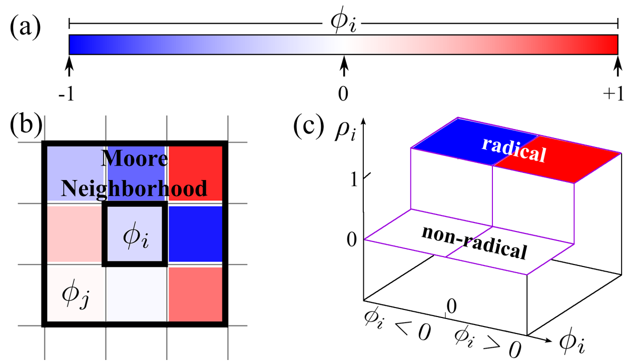

FIG. 2. (a) Schematic of the belief variable $-1 \leq \phi_i \leq 1$. Positive and negative values represent the degrees of belief towards the extreme red and the blue ideologies respectively. The color-coding indicates different values of ϕ_i, with darker colors designated for more zealous beliefs. (b) Definition of nearest neighbors $[i]$. We define nearest neighbors of agent i according to its Moore neighborhood, which include the eight lattice sites surrounding site i. (c) Definition and color-code of radicalization ρ_i. The discrete value of ρ_i is determined via the simplified piecewise constant function in Fig. 1(b). $\rho_i = 1$ represents radicals and is colored red or blue, depending on the corresponding sign of ϕ_i. Non-radicals have $\rho_i = 0$ and are colored white, regardless of their belief value ϕ_i.

distinct attributes. Zealots can be tolerant of the opposite sect and be non-radical. For example, zealots may be deeply religious individuals who at the same time are accepting of others' beliefs.

The site-specific variables ϕ_i and ρ_i depend on each other through an intervening social tension variable σ_i. The basic mechanism for this interplay is that the tension σ_i felt by agent i arises from differences in belief $(\phi_i - \phi_j)$ between agents i and j. In turn, the level of tension σ_i determines the radicalization state ρ_i of agent i, who adjusts its belief ϕ_i accordingly. As mentioned in the Introduction, we will assume ρ_i to be bistable as a function of σ_i. The dynamical model is mathematically described below.

2.2. *Tension and belief adaption.* The tension σ_i perceived by agent i is determined as follows:

$$\sigma_i[\rho(t), \phi(t)] \equiv \sum_{j \in [i]} J(\rho_i, \rho_j)\,(\phi_i - \phi_j)^2\,, \tag{2.1}$$

where the coupling coefficient $J(\rho_i, \rho_j)$ characterizes the sensitivity of agent i with radicalization ρ_i towards the view expressed by agent j with radicalization ρ_j. The sum over j is then taken over Moore neighborhood of i, $[i]$, as shown in Fig. 2(b).

Equation (2.1) allows for tensions to increase when neighbors i and j have different belief levels as modulated by $J(\rho_i, \rho_j)$. By construction, if all sites neighboring i carry the same belief value ϕ_i, the perceived tension $\sigma_i = 0$. The functional dependence of $J(\rho_i, \rho_j)$ will be defined in the Model Parameters Section. Since the maximum of $|\phi_i - \phi_j| = 2$, $0 \leq \sigma_i \leq 32 \max(J)$, where $\max(J)$ is the maximum of $J(\rho_i, \rho_j)$.

The discrete value assigned to ρ_i is determined by the piecewise-constant hysteresis function illustrated in Fig. 1(b) and depends on whether σ_i, determined in equation (2.1), exceeds a "radicalization point" E, is below a "pacification point" D, or lies in between. The bistable dependence of ρ_i on σ_i can be expressed as follows:

$$\rho_i(\sigma_i(t)) \begin{cases} = 1 & \text{if } \sigma_i(t) > E, \\ = 0 & \text{if } \sigma_i(t) < D, \\ \text{unchanged} & \text{otherwise.} \end{cases} \tag{2.2}$$

Since D and σ_i (and consequently J in equation (2.1)) can be rescaled by E; without loss of generality, we can set $E \equiv 1$. Phenomenologically, equation (2.2) allows high tension to drive a non-radical toward radicalization, while low tension may pacify a radical.

We assume the radicalization state ρ_i feeds back to ϕ_i via a modified continuous-time DeGroot model to include contrarian behavior as follows:

$$\frac{\mathrm{d}\phi_i(t)}{\mathrm{d}t} = \sum_{j\in[i]} k(\rho_i, \rho_j, \phi_i, \phi_j)\,(\phi_j - \phi_i)\,. \tag{2.3}$$

Here $k(\rho_i, \rho_j, \phi_i, \phi_j) > 0$ is the rate of change of belief of ϕ_i towards or away from ϕ_j. A positive value of k implies social conformity behaviors that prompt ϕ_i to converge to ϕ_j. A negative value of k represents "contrarian behaviors" where ϕ_i drifts away from ϕ_j. The functional dependence of $k(\rho_i, \rho_j, \phi_i, \phi_j)$ will be defined in the Model Parameters Section.

Note that equation (2.3) can also be written in the form $\phi_i(t + \mathrm{d}t) = \sum_j M_{ij}\phi_j(t)$, where $M_{ij} = k(\rho_i, \rho_j, \phi_i, \phi_j)\mathrm{d}t$ for $j \in [i]$, and $M_{ii} \equiv (1 - \sum_{j\in[i]} k(\rho_i, \rho_j, \phi_i, \phi_j))\mathrm{d}t$. For discrete-time DeGroot models $\mathrm{d}t = 1$ and the matrix $\mathbf{M}$ is known as the "trust matrix" satisfying $\sum_j M_{ij} = 1$. To prevent $\phi_i(t)$ from exceeding the bounds, we further implement no flux boundaries by requiring $k \to 0$ at $\phi_i = \pm 1$. This implementation is consistent with the inflexibility of zealous beliefs assumed in a previous q-voter model [26].

The rules governing the belief value ϕ_i, the intolerance level ρ_i, and the perceived tension σ_i, are given by equations (2.3), (2.2), and (2.1), respectively. With initial conditions and definitions of the parameter functions $J(\rho_i, \rho_j)$ and $k(\rho_i, \rho_j, \phi_i, \phi_j)$ in the next section, these equations fully define our bistable belief and radicalization dynamics model.

2.3. *Model parameters.* In this subsection, we define how $J(\rho_i, \rho_j)$ and $k(\rho_i, \rho_j, \phi_i, \phi_j)$ depend on the relevant variables and then determine the number of independent parameters of the model. We first discuss the coupling function $J(\rho_i, \rho_j)$ and assume that interactions with or between radicals heighten the sensitivity towards belief diversity, resulting in higher social tension. We thus assign

$$J(\rho_i, \rho_j) = \begin{cases} J_- & \text{if } \rho_i = \rho_j = 0, \\ J_+ & \text{otherwise,} \end{cases} \tag{2.4}$$

where $J_+ \geq J_- \geq 0$ quantify high and low sensitivities respectively.

For the rate of change of belief presented in equation (2.3), it is required that $k(\rho_i, \rho_j, \phi_i, \phi_j) \to 0$ at $|\phi_i| = 1$ to prevent ϕ_i from exceeding the bounds. For $|\phi_i| < 1$, we set $k(\rho_i, \rho_j, \phi_i, \phi_j) = \pm 1$ to most simply describe conformation and dissension. If agent i finds the belief of its neighbor j agreeable, ϕ_i "ferromagnetically" adjusts towards ϕ_j at the rate $k(\rho_i, \rho_j, \phi_i, \phi_j) = 1$. Conversely, if neighbor j antagonizes agent i, $k(\rho_i, \rho_j, \phi_i, \phi_j) = -1$ and ϕ_i shifts away from ϕ_j, resulting in an "antiferromagnetic" behavior. Finally we assume the following qualitatively reasonable rules to determine whether belief conformation or dissension occurs.

(1) A non-radical ($\rho_i = 0$) conforms to the beliefs of neighboring non-radicals but dissents from the beliefs of radicals ($\rho_j = 1$), regardless of their belief ϕ_j of the neighbors. In this case

$$k(\rho_i, \rho_j, \phi_i, \phi_j) = \begin{cases} 1 & \text{if } \rho_i = 0 \quad \text{and } \rho_j = 0, \\ -1 & \text{if } \rho_i = 0 \quad \text{and } \rho_j = 1. \end{cases} \tag{2.5}$$

(2) A radical conforms to the beliefs of neighbors of the same sect and dissents from the beliefs of neighbors of the opposite sect, regardless of their radicalization level. In this case

$$k(\rho_i, \rho_j, \phi_i, \phi_j) = \begin{cases} 1 & \text{if } \rho_i = 1 \quad \text{and } \phi_i\phi_j \geq 0, \\ -1 & \text{if } \rho_i = 1 \quad \text{and } \phi_i\phi_j < 0. \end{cases} \tag{2.6}$$

The above assignment of $k(\rho_i, \rho_j, \phi_i, \phi_j)$ is summarized in Table 1 and illustrated in Fig. 3. The discontinuity of $k(\rho_i, \rho_j, \phi_i, \phi_j)$ at $|\phi_i| = 1$ can be made continuous by setting $k(\rho_i, \rho_j, \phi_i, \phi_j) = \pm\left[1 - \tanh((|\phi_i| - 1)/\epsilon)/2\right]$ with an infinitesimal parameter $\epsilon \ll 1$. For numerical simulations, we may choose ϵ to be the same order of magnitude as the time step size.

Table 1. Table listing the values of $k(\rho_i, \rho_j, \phi_i, \phi_j)$, depending on ρ_i and ρ_j, as well as ϕ_i and ϕ_j.

ϕ_i, ρ_i / ϕ_j, ρ_j	$\phi_i > 0$, $\rho_i = 1$	$\phi_i > 0$, $\rho_i = 0$	$\phi_i < 0$, $\rho_i = 1$	$\phi_i < 0$, $\rho_i = 0$
$\phi_j > 0$, $\rho_j = 1$	$+1$	-1	-1	-1
$\phi_j > 0$, $\rho_j = 0$	$+1$	$+1$	-1	$+1$
$\phi_j < 0$, $\rho_j = 1$	-1	-1	$+1$	-1
$\phi_j < 0$, $\rho_j = 0$	-1	$+1$	$+1$	$+1$

Note that $k(\rho_i, \rho_j, \phi_i, \phi_j)$ need not be symmetric with respect to the interchange of i and j since individual i's reaction toward individual j will in general be different from that of j's toward i. This is a major difference between human interactions and physical interactions, which are typically symmetric.

With the definition of $J(\rho_i, \rho_j) = J_\pm$ and $k(\rho_i, \rho_j, \phi_i, \phi_j) = \pm 1$, our equations now have three independent constant parameters: D, J_+ and J_-. Other adjustable parameters not in the equations include the size N of the periodic lattice and the initial

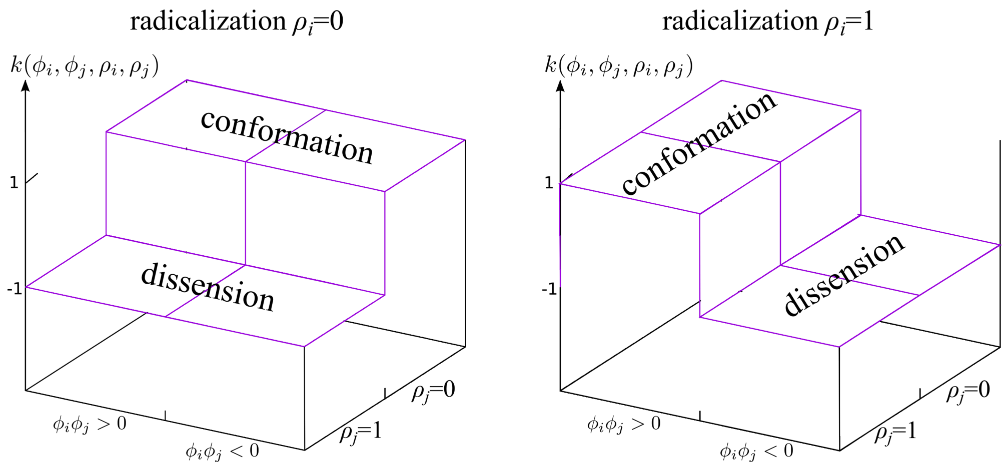

FIG. 3. An illustration of the functional dependence of the belief evolution rate $k(\rho_i, \rho_j, \phi_i, \phi_j)$. Depending on ρ_i, radicals and non-radicals choose conformation ($k = 1$) and dissension ($k = -1$) behavior differently. Non-radicals ($\rho_i = 0$, left panel) determine k based on ρ_j; radicals ($\rho_i = 1$, right panel) determine k based on the sign of $\phi_i\phi_j$, i.e., whether individual j belongs to the same sect as individual i.

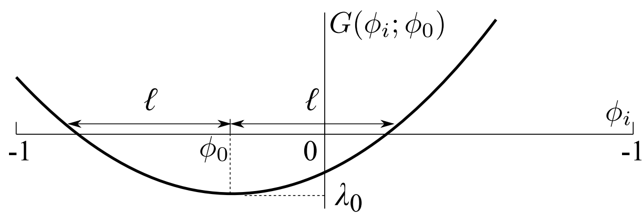

FIG. 4. A global institutional influence function $G(\phi_i; \phi_0)$. The function is defined by three parameters: the institutional stance of belief ϕ_0, the intensity of the influence λ_0, and the breadth of institutional messages ℓ. For $\phi_0 - \ell < \phi_i < \phi_0 + \ell$, $G(\phi_i; \phi_0) < 0$ and the tension σ_i decreases. However, outside this range, σ_i increases.

conditions. We vary the initial red-to-blue population ratio, which we denote as $R(0)$, and unless specified otherwise, we set $J_- = 0.03$, $J_+ = 0.6$, $D = 0.1$, $R(0) = 3/7$ and $N = 100$ as our default parameter values for simulations of equations (2.1)-(2.3). These values are chosen based on our extensive parameter sweep as described in the Results and Discussion sections.

2.4. *Institutional influence.* While the basic model (equations (2.1)-(2.3)) describes the spread of radicalization, we may also wish to include intervention strategies that may alleviate conflict. Historically, a more peaceful coexistence of divided populations is facilitated by the presence of a strong or influential central figure, such as the state, a dictator, inter-communal institutions, or the international community [7, 11, 17, 32]. While such a central figure can influence various facets of a society, in this paper we mainly consider how the outreach of government institutions affects social tension.

We model a governmental institution as a globally connected player that adopts a stance ϕ_0 on the belief scale [31]. Institutional publicity or incentives may appease individuals holding similar beliefs to ϕ_0, causing a reduction of the social tension they perceive. However, for individuals with significantly different beliefs compared to ϕ_0, the perceived tension may increase. We model the influence of the institutions on the social tension perceived by agent i via a simple three-parameter quadratic function

$$G(\phi_i) = \frac{\lambda_0}{\ell^2} (\phi_i - \phi_0)^2 - \lambda_0, \tag{2.7}$$

as plotted in Fig. 4. We thus impose that under governmental influence, the social tension obeys the following

$$\sigma_i[\rho(t); \phi(t)] = \sum_{j \in [i]} J(\rho_i, \rho_j) (\phi_i - \phi_j)^2 + G(\phi_i; \phi_0). \tag{2.8}$$

The constant λ_0 represents the intensity of the institutional influence and is proportional to, say, the available resources and invested efforts. The half distance ℓ between the two x-axis intercepts characterizes the breadth of the institutional message as shown in Fig. 4. Within the range $\phi_0 - \ell < \phi_i < \phi_0 + \ell$, $G(\phi_i) < 0$. Here the institutional message is assumed to be appeasing to individual i, leading to the reduction of its social tension σ_i. However, individuals with beliefs outside of this range will experience an increased tension.

For simplicity, we assume that the institutional stance ϕ_0 does not directly sway a belief ϕ_i, leaving equations (2.2) and (2.3) intact. It is important to note that in general an institution may indirectly steer the beliefs of a general population towards its stance by reducing social tensions and thus encouraging conformity towards its stance ϕ_0. For simplicity, we do not consider this case.

In the following section, we first identify the scenarios that lead to the spread of radicalization in the basic model equations (2.1)-(2.3) without institutional influence. We then include such institutional influence by replacing equation (2.1) with equation (2.8) and explore the outcomes.

3. Results and discussion. We first examine the basic model equations (2.1)-(2.3) without institutional influence to investigate the dependence of ϕ_i and ρ_i on the five adjustable parameters: J_+, J_-, D, N, and $R(0)$. Simulations of the basic model are carried out by numerically integrating equations (2.1)-(2.3) using a semi-implicit method to update the levels of belief ϕ_i and radicalization ρ_i. The numerical discretization is detailed in the Appendix.

The initial conditions of the simulation were set at $\rho_i = 0$ and by randomly drawing values of ϕ_i from a uniform distribution. We further rebalanced ϕ_i such that the $\phi_i > 0$ to $\phi_i < 0$ (red-to-blue) ratio was $R(0) = 3/7$. Next, we placed a radical agent ($\rho^* = 1$) with belief $\phi^* = 0.9$ at the center of the lattice. For the rest of the paper, $\rho^* = 1$ and $\phi^* = 0.9$ will be used as the initial values of the radical agent at the center of the lattice if such a seed is planted. The results are qualitatively similar for sufficiently extreme values of ϕ^*

($\phi^* \gtrsim 0.9$ or $\phi^* \lesssim -0.9$). Uncertainty however rises with smaller $|\phi^*|$ as the radical seed tends to be increasingly pacified at the onset of our simulations. A snapshot of ϕ_i and ρ_i at $t = 1$ is shown in Figs. 5(a) and (b), respectively, and the default parameter values are used for the simulation. Note that by normalizing $|k(\rho_i, \rho_j, \phi_i, \phi_j)|$ our simulation time t is defined on the belief-changing time scale. In Fig. 5(a) we use the color codes in Fig. 2(a) to depict ϕ_i for each individual i, with darker red/blue colors representing more extreme views among the respective sects. In Fig. 5(b) we plot the corresponding ρ_i using the color codes in Fig. 2(c), where radicals are marked by red/blue grids and non-radicals white. As can be seen, radicals tend to exhibit a more extreme level of belief than non-radicals. The latter mostly conform toward relatively neutral beliefs if not in contact with radicals. However, one can still see darker spots in Fig. 5(a) in the regions corresponding to non-radical sites in Fig. 5(b). This shows that regions in which zealots are not radicalized can be sustained, and peaceful coexistence can be achieved. During the simulation, non-radicals can be radicalized by their radical neighbors, leading to an outward spread of radicalization from the initially planted radical seed. Considering that radicalization often precedes conflicts, this "contagion" effect may be referred to as "escalation diffusion" of conflicts, which was identified as a dominant mechanism driving the spread of conflicts [30].

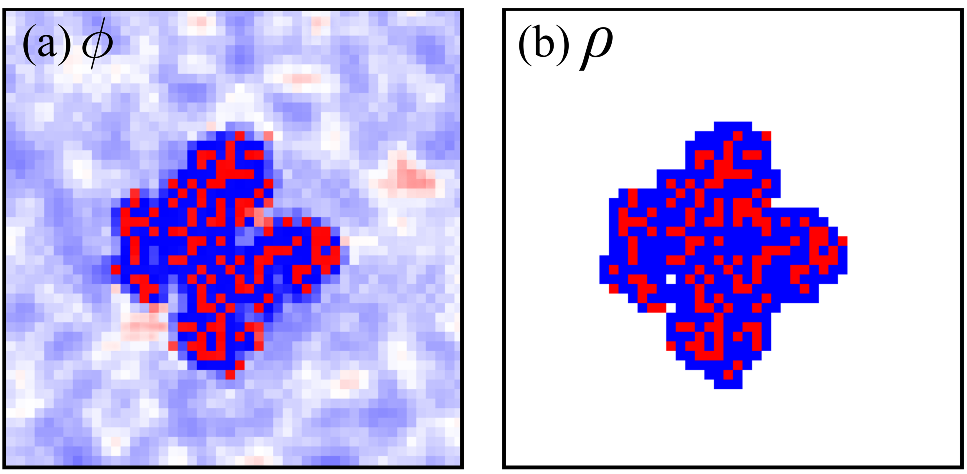

Fig. 5. A snapshot of the spatial distribution of (a) ϕ_i and (b) ρ_i during a simulation. (a) The color-codes (see Fig. 2(a)) reflect the intensity level of belief ϕ_i, with red and blue indicating the two opposing opinions. (b) The corresponding radicalization values ρ_i using the color-codes in see Fig. 2(c). The simulation is initiated with $\rho_i = 0$ and values of ϕ_i randomly drawn from a uniform distribution such that $R(0) = 3/7$. A radicalized agent with $\rho^* = 1$ and $\phi^* = 0.9$ is seeded at the center of the lattice, which triggers the spread of a radicalized population. The simulation is conducted on a 100×100 lattice, but the images here are cropped to better show the radicalized population at the center. The other parameters are set to the default values listed in Sec. 2.3.

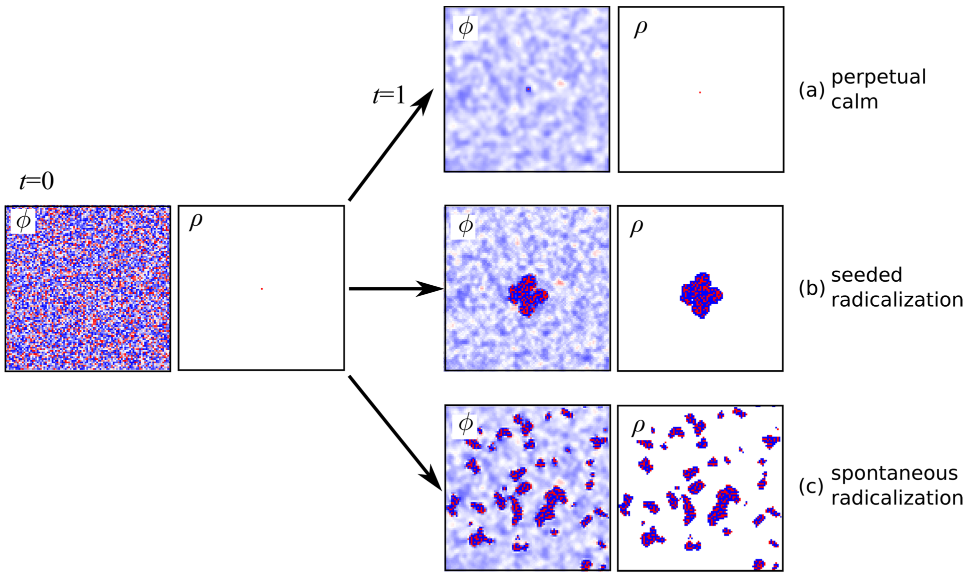

FIG. 6. Three typical evolutions of the model equations (2.1)-(2.3): (a) a perpetual calm situation ($J_- = 0.01$, $J_+ = 0.1$), (b) seeded radicalization ($J_- = 0.03$, $J_+ = 0.6$), and (c) spontaneous radicalization ($J_- = 0.06$, $J_+ = 0.4$). The left panel shows the initial conditions of ϕ and ρ with a radical seed at the center of the lattice. In the perpetual calm situation, the radical seed is unable to radicalize anyone else. In the scenario of seeded radicalization, a radical population spreads out from the initially seeded radical through nearest-neighbor interactions. For spontaneous radicalization, individuals radicalize even in the absence of direct contact with other radicals. The other parameters of these simulations are $D = 0.1$, $R_0 = 3/7$, and $N = 100$.

This scenario can also be described as "heterogeneous nucleation" of an "antiferromagnetic" phase within the context of solid state physics [3]. In addition our model can also lead to other qualitatively different dynamics, as displayed in Fig. 6. Indeed, the behaviors shown in Fig. 6 summarize all possible outcomes from our model under different parameter choices and initial conditions, as confirmed by extensive simulations. Using the same initial conditions as in Fig. 5 but choosing $J_- = 0.01, J_+ = 0.1,$) depicts a peaceful situation where ϕ_i converges towards a consensus value throughout the lattice except near the initially planted radical. Although its neighboring agents become zealots, as shown by the darker blue colors in Fig. 6(a), they remain non-radical and prevent radical attitudes from spreading. We refer to this outcome as one of "perpetual calm". Fig. 6(b) displays the same results as in Fig. 5 for $J_- = 0.03$ and $J_+ = 0.6$. We denote this behavior as "seeded radicalization". Finally, in Fig. 6(c), the parameters $J_- = 0.06, J_+ = 0.4$ lead to a hypersensitive system where non-radicals can spontaneously radicalize. Clusters of high tension "antiferromagnetic" domains spontaneously arise in a manner similar to homogeneous nucleation. We call this type of response "spontaneous radicalization". These three scenarios comprise all qualitatively distinct outcomes of the model seeded with a radical agent at the center of the lattice.

To quantitatively compare the three qualitatively different outcomes shown in Fig. 6, we compute

$$
\begin{aligned}
&\text{(a) mean radicalization:} && \bar{\rho}(t) = \frac{1}{N^2}\sum_i \rho_i(t),\\
&\text{(b) } \tfrac{(\phi>0)}{(\phi<0)} \text{ (red:blue) ratio:} && R(t) = \frac{\sum_i H(\phi_i)}{\sum_j H(-\phi_j)},\\
&\text{(c) mean belief value:} && \bar{\phi}(t) = \frac{1}{N^2}\sum_i \phi_i(t),\\
&\text{(d) polarity of belief:} && P(t) = \frac{1}{N}\sqrt{\sum_i (\phi_i(t) - \bar{\phi}(t))^2},
\end{aligned}
\tag{3.1}
$$

where $H(x) = 1$ for $x > 0$ and 0 otherwise is the Heaviside function. Here, $\bar{\rho}(t)$ measures the population fraction of radicals, $\bar{\phi}(t)$ can be interpreted as a consensus belief, and $P(t)$ is the standard deviation of belief.

Fig. 7(a) shows the radical fraction $\bar{\rho}(t)$ as a function of time. For the case of perpetual calm (solid curve), none of the non-radical agents are turned radical by the planted radical seed, and $\bar{\rho}(t) = 1/N^2$ throughout the simulation. If the sensitivity $J_\pm$ to different neighboring beliefs is increased, radicalization can spread radially from the radicalized seed. The thin dashed curve in Fig. 7(a) shows that the area fraction increases quadratically with time, implying that the typical length scale of the "antiferromagnetic" radicalization phase increases linearly in time. If the minimum sensitivity J_- is further increased, tension between neighboring non-radicals with different beliefs is not low enough to prevent spontaneous radicalization. In this case, $\bar{\rho}(t)$ (dotted curve) rises quickly to its maximum of unity.

Fig. 7(b) plots the evolution of the red-to-blue population ratio $R(t)$. In the case of perpetual calm, belief conformity prompts all agents to join the majority blue sect. In the other two cases, the minority red sect members initially conform to the blue ideology. However, once the number of radicals increase, some blue non-radicals become alienated by blue radicals and are driven towards a more red belief, progressively turning into red radicals.

Fig. 7(c) shows that under calm conditions the average opinion $\bar{\phi}(t)$ remains constant. Under these conditions $k(\phi_i, \phi_j, \rho_i, \rho_j)$ is symmetric for every i-j pair and $\mathrm{d}\bar{\phi}/\mathrm{d}t = 0$. The value of $\bar{\phi}(t) = -0.2$ is thus set by the initial red-to-blue ratio $R(0) = 3/7$. For the two radicalization scenarios, the increasing number of radicals that adopt extreme beliefs causes $\bar{\phi}(t)$ to deviate from $\bar{\phi}(t = 0)$.

Finally, in Fig. 7(d) the polarity $P(t)$ shows convergence of ϕ_i towards a consensus belief in the case of perpetual calm. This is typical for canonical DeGroot models, except that the planted radical seed prevents $P(t)$ from vanishing asymptotically. In the case

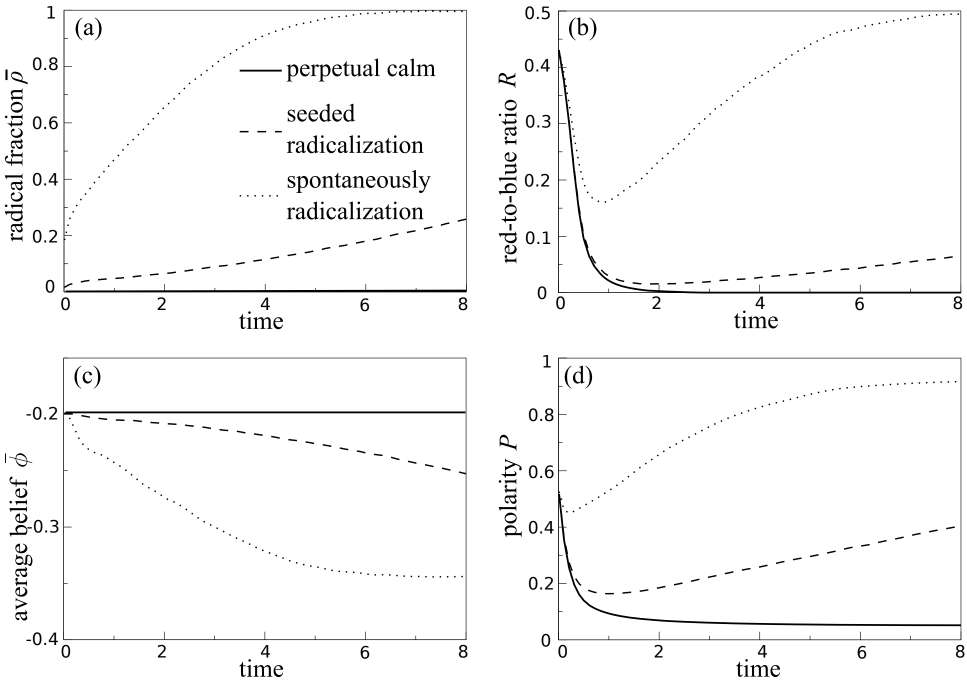

Fig. 7. Time series of (a) radical fraction $\bar{\rho}(t)$, (b) red-to-blue population ratio $R(t)$, (c) mean belief value $\bar{\phi}(t)$, and (d) polarity of belief $P(t)$ for the scenarios of perpetual calm (solid curves), seeded radicalization (dashed curves), and spontaneous radicalization (dotted curves). The parameters for each of the three scenarios are the same as in Fig. 6. For the perpetual calm situation, decreasing P indicates that the belief values ϕ_i conform to a consensus. The latter is achieved by the red (minority) population converting to blue, as demonstrated by the decreasing $R(t)$. In the other two scenarios, the emergence of radicals eventually causes ϕ_i to deviate from the consensus, leading to high P. Many blue individuals who remain non-radical are antagonized by the emerging radicals, most of which are blue, and thus pushed towards red beliefs, leading to a rising trend of $R(t)$.

of seeded radicalization (dashed curve), $P(t)$ initially decreases due to fast conformity followed by a slower increase during which radicalization spreads. If radicalization is spontaneous, the initial conformation phase of decreasing $P(t)$ is overcome by a more rapid radicalization rate that leads to larger polarity.

We find that the sensitivity of non-radicals J_- is the primary determinant of whether spontaneous radicalization emerges or not. In Fig. 8(a), we plot radical fractions versus J_- for several values of J_+ at a long time after initiation ($t = 50$) to identify the parameter regimes where spontaneous radicalization arises. Initial conditions are set at $\sigma_i = 0$ and a randomly distributed $-1 \leq \phi_i \leq 1$ with $R(0) = 3/7$. No radical agents are planted at $t = 0$. In the absence of a radical seed, non-radicals become radicalized exclusively through the tensions arising from belief differences amongst themselves. We find that spontaneous radicalization is triggered for $J_- > 0.04$ and that this threshold does not depend on J_+. For low values of $J_+ \lesssim 0.2$, the spread of radicals can be arrested after the emergence of spontaneously radicalized patches. As a result, radicals do not pervade society even at long times.

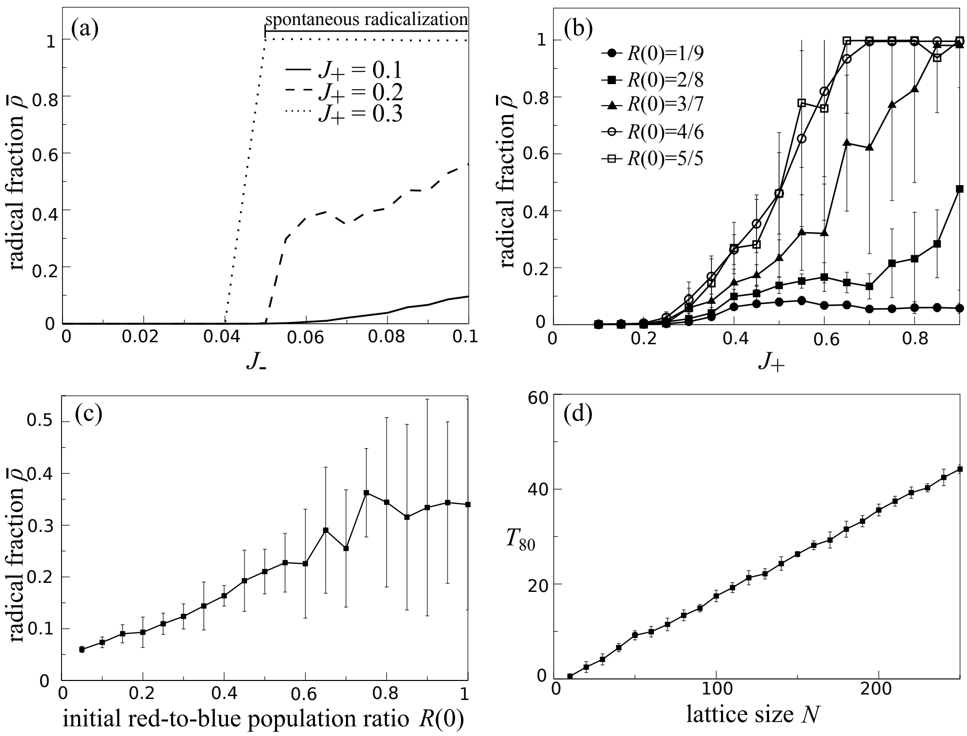

Fig. 8. Parameter dependence of the basic model (equations (2.1)-(2.3)). (a) Spontaneous radicalization triggered by increasing J_-. Long-time ($t = 50$) radical fractions of simulations without initial radical seeds are plotted against J_- for various J_+ values. When J_- exceeds a threshold, non-radicals spontaneously radicalize. For long enough time and sufficiently large J_+, the spontaneously emerging radicals spread through the entire population. (b) Spread of seeded radicalization regulated by J_+. Radical fractions at an intermediate time ($t = 10$) are plotted against J_+ for various $R(0)$ ratios. A larger J_+ causes radicals to spread faster, reaching a higher radical fraction at an intermediate time. (c) Intermediate-time ($t = 10$) radical fraction versus $R(0)$ for $R(0) \leq 1$. More closely matched initial red and blue populations also result in faster spread of radicals. (d) Time for the radicalization cluster to reach 80% of the system area for various lattice domain size N in the presence of an initially planted radical at the center of the lattice. The time increases linearly with N, suggesting a linear radial expansion of the cluster over time. If not varied in the figures, the default parameters values are used. An initial radical seed is planted for Figures (b)-(d) but not (a). Each data point represents the mean value of ten simulations, and error bars the standard deviations.

Henceforth, we plant a radical seed at the center and set $J_- = 0.03$ to focus on seeded radicalization, a qualitatively reasonable description of the nucleation and growth of sectarianism. Recalling that $\sigma_i \leq 32\max(J)$, we have $\sigma_i \leq 0.03 \times 32 = 0.96 < 1$ if $J = J_-$ everywhere, eliminating the chance of spontaneous radicalization. As long as $J_- < 1/32$, spontaneous radicalization cannot arise. In Fig. 8(b), we plot radical fractions $\bar{\rho}(t = 10)$ as a function of J_+ for various initial red-to-blue ratios $R(0)$. Radicals begin to spread from the planted seed when $J_+ > 0.25$ regardless of $R(0)$. For larger J_+, the radicalization cluster reaches a larger fraction of the lattice indicating a faster spreading rate. A larger initial ratio $R(0)$ also causes the cluster of radicals to spread at a faster rate. This is confirmed in Fig. 8(c) where radical fraction $\bar{\rho}(t = 10)$ for $J_+ = 0.6$ increases with $R(0)$, and is maximal for $R(0) \gtrsim 0.75$, where the members of the two sects are about equal.

These findings are consistent with the observation that conflicts mostly arise in regions where ethnic boundaries are not well-defined (i.e., a mixed population) and where the populations of ethnic groups are closely matched [24]. A minority population that is overwhelmed by a much more populous opposing belief more easily assimilates and is less likely to elicit conflict. An example can be found in Indonesia, where analysis of survey data suggested that the spread of radical beliefs was subdued in villages consisting of a notably dominant majority population [4].

In Fig. 8(d) we plot the time T_{80} for the radicalization cluster to cover 80% of the lattice, which for our simulations corresponds roughly to the time it takes for the cluster perimeter to reach the boundaries of the lattice. We find that T_{80} increases linearly with domain size N, suggesting that the radius of the radicalized cluster area grows linearly with time, and that the corresponding area scales as t^2, consistent with Fig. 7(a).

Finally, we find that tension σ_i rarely decreases among a mixed population, precluding de-radicalization. As a consequence, we find that the value of the pacification point D in Fig. 1(b) has essentially no effect on seeded radicalization in our basic model equations (2.1)-(2.3).

3.1. *Global institutional influence.* So far we have investigated the parameter dependence of the basic model equations (2.1)-(2.3). We now explore how an external institutional influence may affect radicalization. We set the basic model parameters to the default values ($J_- = 0.03$, $J_+ = 0.6$, $D = 0.1$, $R(0) = 3/7$, and $N = 100$) and focus on the fast seeded radicalization regime, shown in Fig. 6(b) in the absence of any external players. We here add a global institutional influence $G(\phi_i; \phi_0)$ by replacing equation (2.1) with equation (2.8).

In Fig. 9(a) we plot the long-time ($t = 50$) radical fraction $\bar{\rho}(t = 50)$ and examine the effect of λ_0, which defines the intensity of the tension-reducing influence. We choose $\phi_0 = 0$ and $\ell = 1$, so that the external institution adopts a neutral stance and reduces perceived tension for individuals with any belief value ϕ_i. For these parameters, we observe significant and consistent reduction of radical fractions when $\lambda_0 \gtrsim 1.6$. For $\lambda_0 \gtrsim 2.5$, the spread of radicals by the seed is largely suppressed. Hence, one of our major findings is that to exert significant influence λ_0, the institutional influence needs to have a high penetration within the overall population.

In Fig. 9(b), the radical fraction $\bar{\rho}(t = 50)$ is depicted using a color intensity map and plotted as a function of ℓ and λ_0. As expected, the lowest radicalization levels are achieved by large λ_0 and ℓ, indicating that for a strong influence intensity to pacify conflicts, the institutional publicity must also have broad appeal. Note that in realistic situations the institutional influence intensity and message breadth are often constrained by the resources available to the institution. It may thus become impractical to simultaneously achieve high penetration and broad appeal given limited resources. How to most effectively allocate resources is an interesting optimization problem.

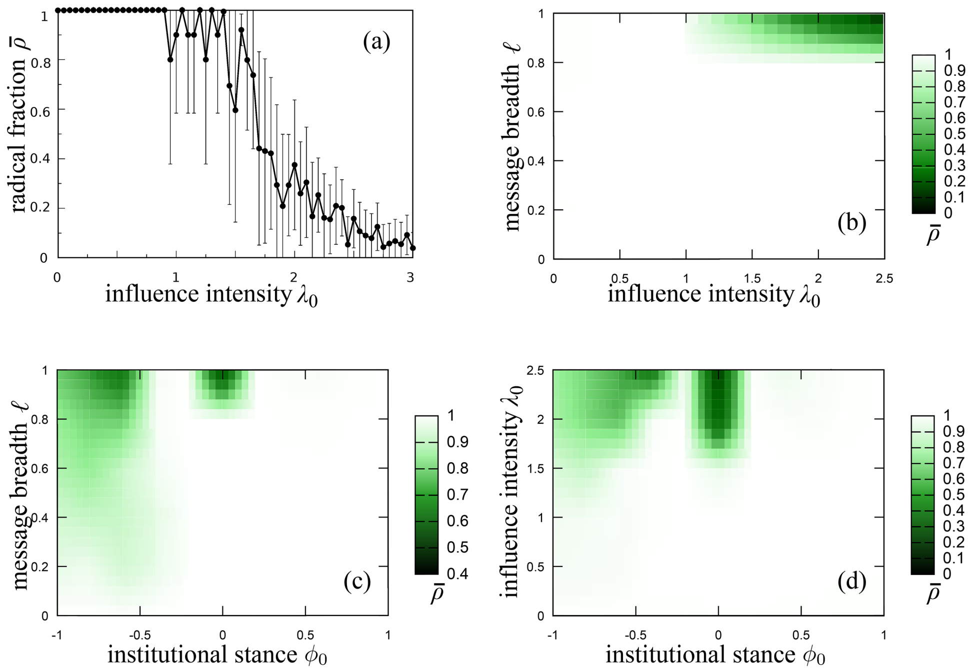

Fig. 9. (a) Reduction of radical fraction for various strengths of global institutional influence λ_0. We plot long-time ($t = 50$) radical fractions versus λ_0 while setting the institutional stance $\phi_0 = 0$ and message breadth $\ell = 1$. When $\lambda_0 \gtrsim 1.6$, the institutional influence begins to show a significant effect, and radicals have mostly stopped spreading when $\lambda_0 \gtrsim 2.5$. (b) Long-time ($t = 50$) radical fractions as a function of ℓ-λ_0, (c) ℓ-ϕ_0, and (d) λ_0-ϕ_0. The color maps represent radical fractions. For (b) the institution adopts a neutral stance $\phi_0 = 0$. The most reduction of radicals is achieved at high λ_0 and large ℓ. For (c), we set $\lambda_0 = 2$. A neutral (ϕ_0) and a majority-biased stance ($\phi_0 \sim -0.5$) both register significant reduction of radicals. For (d) we choose $\ell = 1$, and again $\phi_0 = 0$ and $\phi_0 \sim 0.5$ both result in significant reduction of radicals. Each data point represents the mean value of ten simulations, and error bars in (a) indicate the standard deviations.

In Fig. 9(c) we plot $\bar{\rho}(t = 50)$ against ℓ and ϕ_0 with $\lambda_0 = 2$. The largest reduction of radicals occurs in the tongue near the neutral institutional stance $\phi_0 = 0$, but diminishes as ℓ is decreased. Some reduction of radicals is also observed when $-1 < \phi_0 < -0.5$, corresponding to a stance biased toward the majority belief. Although this latter regime $-1 < \phi_0 < -0.5$ does not result in as significant a reduction in radical level as the $\phi_0 \approx 0$ tongue for $\ell \approx 1$, the reduction occurs over a wider range of ℓ. We thus find that if the external institution is unable to fashion a message with sufficiently broad appeal, it may be better to bias its influence to appease the majority.

In Fig. 9(d) we show $\bar{\rho}(t = 50)$ versus λ_0 and ϕ_0 with $\ell = 1$. Again, a neutral institutional stance ($\phi_0 = 0$) achieves the most reduction of radicals, while a majority-biased stance also has some success but to a lesser degree. With respect to influence intensity λ_0, we find that the effectiveness of a majority-biased institutional stance diminishes quickly with decreasing λ_0, while a neutral stance is capable of maintaining a lower radical fraction at a lower λ_0.

Our results suggest that an institutional influence achieves optimal results if the entity carefully adopts a strong but neutral stance between the two conflicting beliefs. However, the outreach of the institutional message content is also important. If the institutional influence targets a narrow range of beliefs for the reduction of perceived tension, it may alienate those out of reach, and may have the opposite effect of increasing radicalization. If the institution is unable to placate population with a wide range of beliefs, a stance favoring the majority view may be an effective alternative. Of course, other mechanisms of external influence may apply. For example, governing institutions may directly influence people's beliefs rather than just the tension they perceive. To model such mechanisms, a modification of equation (2.3) can be developed.

4. Conclusions. In this paper, we construct a belief dynamics model that incorporates a bistable radicalization process to describe the spread of sectarian conflict. While the model equations can be applied to arbitrary social network structures, we simulate our model on a locally connected two-dimensional square lattice with periodic boundary conditions. By defining belief and radicalization as separate variables, our model allows for a more nuanced description that distinguishes belief from radicalization. Although in the absence of radicals, all non-radicals asymptotically conform to an apathetic/neutral consensus due to the simplicity of the model, we do observe transient enclaves of more zealous but non-radical individuals. Radicals, on the other hand, are mostly zealots with extreme belief values. We examine the parameter dependence of the model and identify regimes leading to three distinct evolution paths. In the regime of perpetual calm, non-radical individuals cannot be radicalized even by planting radical seeds in advance. In the regime of spontaneous radicalization, non-radical individuals may spontaneously radicalize even in the absence of radicals. Between the above two regimes lies the regime of seeded radicalization, where non-radical individuals cannot spontaneously radicalize but can become radical upon contact with other radicals. For subsequent investigations, we choose parameter values in the third regime, as the most realistic scenario for the propagation of sectarian conflicts. We find that radicalization can be suppressed by a numerically more dominant majority population between the two competing sects. Finally we implement institutional influence as a globally connected player and find that the most effective intervention to pacify conflict is to adopt a strong but neutral view.

Our model represents a first step in studying the bistable (or multistable) nature of human behaviors in the development of social conflicts. Our incorporation of bistability is only phenomenological, while the underlying mechanism is a fundamental but much more challenging component to design and include. Moreover, the separation of ideological belief and radicalization that we propose is a simplified version of multi-dimensional opinion dynamics models. Our modeling framework can be extended to include multiple ideological spectrums, such as religion, social economics, and politics, and examine the interplay among them. We can also introduce belief fluctuations and individual migrations to investigate transitions among equilibrium states, such as isolated enclaves and well mixed communities, when parameters are changed or radical seeds are introduced or removed. Finally, our model can be straightforwardly extended to include evolving, non-lattice social networks.

Appendix: Numerical implementation. For numerical simulations, we adopt a semi-implicit method with a fixed time step size to integrate our model. Let us denote $\phi_i(t)$, $\rho_i(t)$, and $\sigma_i(t)$ at a discrete time $t = n\Delta t$ as ϕ_i^n, ρ_i^n, and σ_i^n, where Δt is the time step size. Then we discretize equations (2.1)-(2.3) as

$$\sigma_i^{n+1} = \sum_{j\in \text{n.n.[i]}} J(\rho_i^{n+1}, \rho_j^{n+1}) \left(\phi_i^{n+1} - \phi_j^{n+1}\right)^2, \tag{A1}$$

$$\rho_i^{n+1} = \begin{cases} 1 & \text{if } \sigma_i^{n+1} > 1, \\ 0 & \text{if } \sigma_i^{n+1} < D, \\ \rho_i^n & \text{otherwise}, \end{cases} \tag{A2}$$

$$\phi_i^{n+1} = \phi_i^n + \Delta t \sum_{j\in \text{n.n.[i]}} k(\rho_i^n, \rho_j^n, \phi_i^n, \phi_j^n) \left(\phi_j^n - \phi_i^n\right), \tag{A3}$$

and an iterative method is used to solve the semi-implicit equations (A1)-(A3). The equations with global institutional influence are solved in the same way. Note that for an explicit method, equation (2.2) may impose a severe constraint on Δt, and even with an adaptive time step size, the numerical integration can still be very inefficient.

References

[1] D. Acemoğlu, G. Como, F. Fagnani, and A. Ozdaglar, *Opinion fluctuations and disagreement in social networks*, Math. Oper. Res. **38** (2013), no. 1, 1–27, DOI 10.1287/moor.1120.0570. MR3029476

[2] D. Acemoglu and A. Ozdaglar, *Opinion dynamics and learning in social networks*, Dyn. Games Appl. **1** (2011), no. 1, 3–49, DOI 10.1007/s13235-010-0004-1. MR2800784

[3] C. Baldasseroni, C. Bordel, C. Antonakos, A. Scholl, K. H. Stone, J. B. Kortright, and F. Hellman, *Temperature-driven growth of antiferromagnetic domains in thin-film FeRh*, J. Phys.: Condens. Matter **27** (2015), 256001.

[4] P. Barron, K. Kaiser, and M. Pradhan, *Local conflict in Indonesia: Measuring incidence and identifying patterns*, World Bank Policy Research Paper 3384, 2004.

[5] R. Bhavnani, K. Donnay, D. Miodownik, M. Mor, and D. Helbing, *Group segregation and urban violence*, American Journal of Political Science **58** (2014), 226–245.

[6] R. M. Bozorth, *Ferromagnetism*, IEEE press, New York, 1951.

[7] A. C. Carpenter, *Community resilience to sectarian violence in Baghdad*, Springer-Verlag, New York, 2014.

[8] T. Chapman and P. G. Roeder, *Partition as a solution to wars of nationalism: The importance of institutions*, American Political Science Review **101** (2007), 677–691.

[9] G. Deffuant, D. Neau, F. Amblard, and G. Weisbuch, *Mixing beliefs among interacting agents*, Advances in Complex Systems **3** (2000), 87–98.

[10] M. H. DeGroot, *Reaching a consensus*, Journal of the American Statistical Association **69** (1974), 118–121.

[11] P. Dixon, *Why the Good Friday Agreement in Northern Ireland is not consociational*, The Political Quarterly **76** (2005), 357–367.

[12] S. Eger, *Opinion dynamics under opposition*, http://arxiv.org/abs/1306.3134, 2013.

[13] K. Felijakowski and R. Kosinski, *Bounded confidence model in complex networks*, Internat. J. Modern Phys. C **24** (2013), no. 8, 1350049, 12, DOI 10.1142/S0129183113500496. MR3081417

[14] K. Felijakowski and R. Kosinski, *Opinion formation and self-organization in a social network in an intelligent agent system*, ACTA Physica Polonica B **45** (2014), 2123–2134.

[15] N. E. Friedkin, *Choice shift and group polarization*, American Sociological Review **64** (1999), 856–875.

[16] B. Golub and M. O. Jackson, *Naïve learning in social networks and the wisdom of crowds*, American Economic Journal: Microeconomics **2** (2010), 112–149.

[17] J. Hagan, J. Kaiser, A. R. Hanson, and D. Rothenberg, *Neighborhood sectarian displacement and the battle for Baghdad: A self-fulfilling prophecy of crimes against humanity in Iraq*, http://ssrn.com/abstract=2118775, 2013.

[18] M. A. Javarone, *Social influences in opinion dynamics: The role of conformity*, Physica A **414** (2014), 19–30.

[19] C. Kaufmann, *Possible and impossible solutions to ethnic civil wars*, International Security **20** (1996), 136–175.

[20] U. Krause, *A discrete nonlinear and non-autonomous model of consensus formation*, Communications in difference equations (Poznan, 1998), Gordon and Breach, Amsterdam, 2000, pp. 227–236. MR1792007

[21] R. M. Kunovich and R. Hodson, *Ethnic diversity, segregation, and inequality: A structural model of ethnic prejudice in Bosnia and Croatia*, The Sociological Quarterly **43** (2002), 185–212.

[22] W. F. Lawless, S. Rifkin, D. Sofge, S. H. Hobbs, F. Angjellari-Dajci, L. Chaudron, and J. Wood, *Conservation of information: Reverse engineering dark social systems*, Structure and Dynamics **4** (2010), 1–30.

[23] W. F. Lawless, D. A. Sofge, G. K. Venayagamoorthy, R. Hillson, and C. P. Abubucker, *A physics of interdependence for human-robot-machine organizations*, IEEE International Conference on System of Systems Engineering, 2009, pp. 1–6.

[24] M. Lim, R. Metzler, and Y. Bar-Yam, *Global pattern formation and ethnic/cultural violence*, Science **317** (2007), 1540–1544.

[25] R. MacGinty, *Ethno-national conflict and hate crime*, American Behavioral Scientist **45** (2001), 639–653.

[26] A. Mellor, M. Mobilia, and R. K. P. Zia, *Characterization of the nonequilibrium steady state of a heterogeneous nonlinear q-voter model with zealotry*, Europhysics Letters **113** (2016), 48001.

[27] B. O'Leary and J. McGarry, *The politics of antagonism*, Athlone, London, 1993.

[28] J. Rydgren, D. Sofi, and M. Hällsten, *Interethnic friendship, trust, and tolerance: Findings from two north Iraqi cities*, American Journal of Sociology **118** (2013), 1650–1694.

[29] N. Sambanis, *Partition as a solution to ethnic conflict: Some new hypotheses*, Security Studies **9** (2000), 1–51.

[30] S. Schutte and N. B. Weidmann, *Diffusion patterns of violence in civil wars*, Political Geography **30** (2011), 143–152.

[31] C. Thron, J. Salerno, A. Kwiat, P. Dexter, and J. Smith, *Modeling South African service protests using the national operational environment model*, Social Computing, Behavioral-Cultural Modeling and Prediction (S. Yang, A. Greenberg, and M. Endsley, eds.), no. 298-305, Berlin: Springer, 2012.

[32] N. B. Weidmann and I. Salehyan, *Violence and ethnic segragation: A computational model applied to Baghdad*, International Studies Quarterly **57** (2013), 52–64.

[33] G. Weisbuch, G. Deffuant, F. Amblard, and J.-P. Nadal, *Meet, discuss, and segregate*, Complexity **7** (2002), 55–63.

[34] E. Yildiz, A. Ozdaglar, D. Acemoglu, A. Saberi, and A. Scaglione, *Binary opinion dynamics with stubborn agents*, ACM Transations on Economics and Computation **1** (2013), Article 19.